ELSEVIER

Microcircuits Special Feature

Biophysically detailed modelling of microcircuits and beyond

Erik De Schutter[1], Örjan Ekeberg[2], Jeanette Hellgren Kotaleski[3], Pablo Achard[1] and Anders Lansner[2]

[1]Laboratory of Theoretical Neurobiology, Institute Born-Bunge, University of Antwerp, Universiteitsplein 1, B-2610 Antwerp, Belgium
[2]School of Computer Science and Communication, Royal Institute of Technology and Stockholm University, Lindstedtsvägen 3, SE-10044 Stockholm, Sweden
[3]Department of Neuroscience, Karolinska Institute, SE-17177 Stockholm, Sweden

Realistic bottom-up modelling has been seminal to understanding which properties of microcircuits control their dynamic behaviour, such as the locomotor rhythms generated by central pattern generators. In this article of the *TINS Microcircuits Special Feature*, we review recent modelling work on the leech-heartbeat and lamprey-swimming pattern generators as examples. Top-down mathematical modelling also has an important role in analyzing microcircuit properties but it has not always been easy to reconcile results from the two modelling approaches. Most realistic microcircuit models are relatively simple and need to be made more detailed to represent complex processes more accurately. We review methods to add neuromechanical feedback, biochemical pathways or full dendritic morphologies to microcircuit models. Finally, we consider the advantages and challenges of full-scale simulation of networks of microcircuits.

Introduction

Quantitative computational modelling is becoming an important tool in neuroscience research. Models are developed and studied at all levels, from the molecular processes underlying cellular and synaptic properties to brain-scale neuronal networks. Two complementary modelling strategies are used. 'Bottom-up' simulations start from biophysically realistic models that mimic many details of the system under study and enable open-ended investigation of its properties. 'Top-down' approaches use abstract models or pure mathematics to cast general principles of the system under study into a minimal model, fully describing its essential properties with as few parameters as possible.

The central role of modelling is to promote synthesis of experimental data from different sources into a coherent picture of the system under study. The resulting model can then, for instance, demonstrate how seemingly unexplained phenomena are in fact a consequence of what is already known. Exploration of the model can lead to truly unexpected findings, which then provide important input for the planning of new experiments. In this manner, modelling enables us to extract maximal knowledge from existing data and to find the most promising way ahead.

Bottom-up models have been successful in simulating microcircuits[*] [1,2] (Grillner et al. in this issue) and we first review recent progress made using this approach to simulate the behaviour of two central pattern generators (CPGs), in the leech and the lamprey. Such models traditionally consist of small networks of synaptically connected 'point neurons' (i.e. models without morphology). The active conductances responsible for the excitable properties of the neurons and the synaptic conductances are simulated in a physiologically realistic manner [3]. Mathematical approaches used in top-down modelling have also contributed to better understanding of the two CPGs, but results from these methods are not always congruent with those from the bottom-up approaches. Such differences can be resolved only by intensive interactions between the modellers and experimenters involved. Some authors have advocated combining bottom-up and top-down models for the same system [4], but these techniques are not yet widely used.

In the second part of this review, we consider how one can make the simple network models more elaborate, to increase their realism. We describe simulating neuromechanical feedback, adding biochemical networks involved in synaptic learning, the incorporation of realistic neuron morphology and increasing the size of the network to full-scale (with all neurons modelled). This part uses examples from simulations of the other microcircuits reviewed by Grillner et al. in this *TINS* special feature.
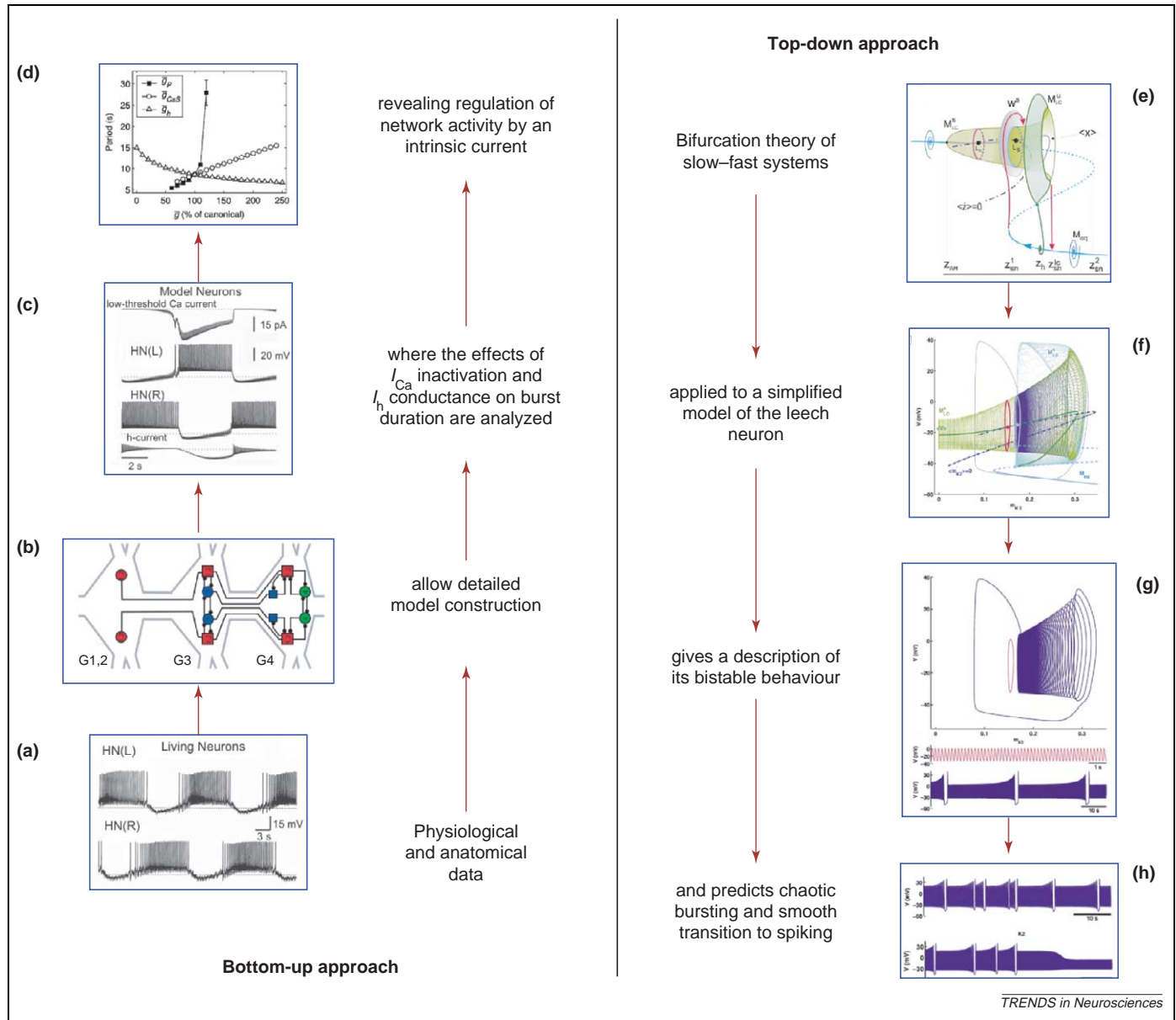
Modelling the leech CPG

Because one can identify individual invertebrate neurons and because their cellular properties and connectivity are stereotypical it is, in principle, possible to create complete

---

[*] In this *TINS* special feature, the term 'microcircuit' is used to denote a minimal number of interacting neurons that can collectively produce a functional output, such as locomotor central pattern generators, hippocampal circuits producing gamma and theta rhythms, and circuits in the neocortex and cerebellum.

models of invertebrate CPGs, replicating all important properties. A system where much progress has been made is the circuit responsible for generating the heartbeat rhythm in the medicinal leech. The sub-circuit of heart interneurons (HN neurons) in the first four segmental

ganglia of the nerve cord (Figure 1b) inhibits segmental motoneurons to control the rhythmic (1 Hz) constrictions of the bilateral heart tubes. The primary foci of oscillation of the CPG are the pairs of HN neurons in the third and fourth ganglia (HN3 and HN4 neurons, respectively),

Figure 1. Two different approaches to modelling the leech heartbeat CPG. On the left (a–d), the models try to reproduce the experimental data as much as possible [6–8]. Afterwards, analyzing the influence of each parameter gives a better understanding of the microcircuit dynamics and leads to new predictions. On the right (e–h), theoretical considerations applied to a simplified model of a HN neuron predict a particular behaviour of this neuron [13]. **(a)** Simultaneous intracellular recordings of the two HN interneurons in ganglion 4. This pair of reciprocally inhibiting neurons forms a half-centre oscillator. **(b)** How the coordinating neurons from the first and second ganglia (G1 and G2) inhibit the half-centre oscillators in the third and fourth ganglia (G3 and G4); the coordinating neurons initiate spikes in their axons in G3 and G4. All synaptic contacts are inhibitory; cell bodies are shown as circles, and additional spike initiation zones are shown as squares; coordinating neurons are in red, HN3 neurons are in blue and HN4 neurons are in green. Note that the HN3 neuron inhibits the coordinating neurons in both G3 and G4, whereas HN4 does so only in G4. **(c)** Fourth-generation model of the segmental half-centre oscillator [7]. Presynaptic low-threshold Ca^{2+} current (upper trace) in HN(L) progressively declines during burst leading to decreased inhibition of the HN(R) neuron. At the same time, amplitude of the hyperpolarization-activated current I_h increases in the HN(R) cell. These two phenomena lead to rebound bursting of the HN(R) neuron, which then inhibits the HN(L) cell. **(d)** Effect of varying the maximal conductances of the intrinsic persistent Na^+ current (g_P), the slow Ca^{2+} current (g_{CaS}), and the hyperpolarization-activated current (g_h) on the period of the elemental oscillator model. **(e)** Bifurcation diagram of a slow–fast system of differential equations. The x-axis represents the slow-phase space variables and the y-axis follows the fast-phase ones. In this singularly perturbed system, the intersection of nullclines gives two periodic orbits: one stable (LN) and one saddle (LS). Any neuron close to LN will be attracted by this point and can therefore follow a stable orbit (red line) corresponding to spiking. Oppositely, LS is attractive in one dimension and repulsive in the other one. In some configurations, neurons around the LS point alternate tonic and silent periods. **(f)** Assuming blockade of Ca^{2+} currents and partial blockade of outward currents, and ignoring persistent Na^+ current, the HN interneuron can be modelled using two currents only: a fast Na^+ current (I_{Na}) and a persistent K^+ current (I_{K2}). The remaining variables are the membrane potential (V), the activation of I_{K2} (m_{K2}) and the inactivation of I_{Na} (h_{Na}). The bifurcation diagram is drawn in the (m_{K2},V) plane. **(g)** Coexistence of spiking (red) and bursting (blue) modes in the model, shown in the (m_{K2},V) plane (top diagram) and with voltage traces obtained from slightly different initial conditions (bottom lines). **(h)** For particular values of $V_{K2shift}$, the shift of membrane potential of half-inactivation of I_{K2} from its canonical value, chaotic bursting (top trace) and smooth transitions between bursting and spiking (bottom) can be observed. Panels (a–d) modified, with permission, from [7,11]; (e–h) modified, with permission, from [13] © (2005) the American Physical Society.

where HN neurons inhibit their contralateral partner. This reciprocal inhibition makes the unstable intrinsic bursting properties of HN neurons more robust [5] and alternating, resulting in a half-centre oscillator behaviour (Figure 1a). A first series of models [6–8] investigated the interaction between the synaptic inhibition, which is both graded and spike-evoked, and the voltage-gated currents in one pair of neurons that form an elemental oscillator. An important and unexpected prediction of the model was that not only the hyperpolarization-activated current I_h, but also slow Ca^{2+} currents that are activated during the burst, would have a strong effect on the period of oscillation (Figure 1c). Of particular importance is how effectively the inhibitory phase removes the inactivation of the Ca^{2+} channels, because this will determine their capacity for activation during the burst phase and the amount of inhibition that can be generated. This prediction was experimentally confirmed when realistic waveforms were used to voltage clamp HN neurons [9], which led to further improvements of the model [7].

The pairs of HN neurons in the first and second ganglia link the oscillators in the third and fourth ganglia through inhibitory synapses (Figure 1b) and are therefore called coordinating interneurons. Their role was investigated in more recent models [10,11]. The bottom-up approach, using previously developed models as building blocks to create larger network models, worked in this case because a relatively realistic six-neuron segmental circuit could be produced by adding simple models of four coordinating interneurons to one elemental oscillator circuit. Spike-mediated inhibition from coordinating interneurons increased the oscillation period but the oscillation behaviour did not change qualitatively [10].

When this model was expanded to the full eight-neuron circuit (Figure 1b), it replicated the phase relationships between HN3 and HN4 neurons when spontaneously entraining each other under 'natural' (closed loop) conditions [10], but not when the CPG was driven by current injection in one neuron (an open loop) [12]. This problem was solved using a more detailed model [11], which explored whether the phase differences are due to an asymmetry in synaptic coupling or to a difference in cellular excitability leading to different intrinsic oscillation frequencies of the elemental oscillators. A similar question dominated the lamprey CPG field for a long time. The bottom-up leech modelling [11] demonstrates that both mechanisms can contribute, depending on the experimental condition. In the closed-loop condition, higher excitability of the HN3 neurons dominates, whereas in the open-loop condition, behaviour is determined by the asymmetry of the circuit (HN3 neurons inhibit the coordinating neurons more than HN4 neurons do; Figure 1b).

More recently, the leech CPG has also been the subject of extensive top-down mathematical analysis that investigated in more detail the transition from tonic to bursting spiking in isolated neurons [13] (Figure 1e–h), as was observed in earlier experimental studies [5]. The approach used was to reduce the complexity of the HN model by blocking or ignoring several active conductances so that it could be reduced to three variables, with one differential equation for each. Bifurcation theory [14] (Figure 1g) enabled Shilnikov et al. to show that a single variable, the half-inactivation of a persistent K^+ current, controls the distance between the attraction domains for tonic spiking and for bursting [13] (Figure 1e). Again these predictions are amenable to experimental study.

Modelling the lamprey spinal pattern generator
The lamprey spinal locomotor system [1,15] generates a wave of neural activity along the body during swimming, normally travelling in the head-to-tail direction but reversed during occasions of backward swimming. It comprises two main types of premotor interneurons, in addition to the motoneurons driving the swimming muscles: ipsilaterally projecting excitatory glutamatergic interneurons, and contralaterally projecting glycinergic inhibitory interneurons (see Grillner et al. in this issue for a circuit diagram). The burst-generating network is extended in the rostrocaudal direction such that the excitatory interneurons project a few segments rostrally and caudally whereas the crossed inhibitory interneurons can extend up to 20 segments caudally. This connectivity is responsible for intersegmental coordination and propagation of the locomotor activity wave along the body. The crossed inhibition is mainly responsible for the left–right alternation of locomotor activity.

Many aspects of the lamprey CPG have been studied using biophysically-detailed modelling, including segmental-burst-generating mechanisms [16,17], steering [18] and plasticity [19]. Recently, a fundamental shift in our understanding of this system has occurred. It started with early modelling results using top-down connectionist models of recurrent excitatory networks. This demonstrated that a network of mutually exciting and adapting interneurons by itself (Figure 2c), in the absence of any inhibition, would be capable of rhythm generation in the locomotor frequency range [20]. This hypothesis was subsequently elaborated by simulating biophysically more detailed models [17]. The predictions were recently confirmed by intricate experiments involving longitudinal transection of the lamprey spinal cord [21,22] (Figure 2a,b). These findings challenge the traditional view of vertebrate locomotor rhythm generation as based on half-centre oscillators, in which reciprocal inhibition is necessary for oscillations to occur (Figure 1b).

The intersegmental coordination during locomotion has also been modelled extensively. The lamprey maintains approximately one wavelength of curvature along its body when swimming, independent of swimming speed [15]. Thus, the lag between burst onsets in consecutive segments constitutes a constant fraction of the cycle duration (referred to as a constant phase lag), independent of cycle duration, at least in the intact animal. Intersegmental coordination is also flexible: in vitro experiments have demonstrated that an isolated piece of spinal cord can be stimulated selectively such that it displays coordination corresponding to either forward or backward swimming [23].

The properties of the microcircuitry responsible for the constant phase lag have been the topic of extensive discussion between bottom-up and top-down modellers.
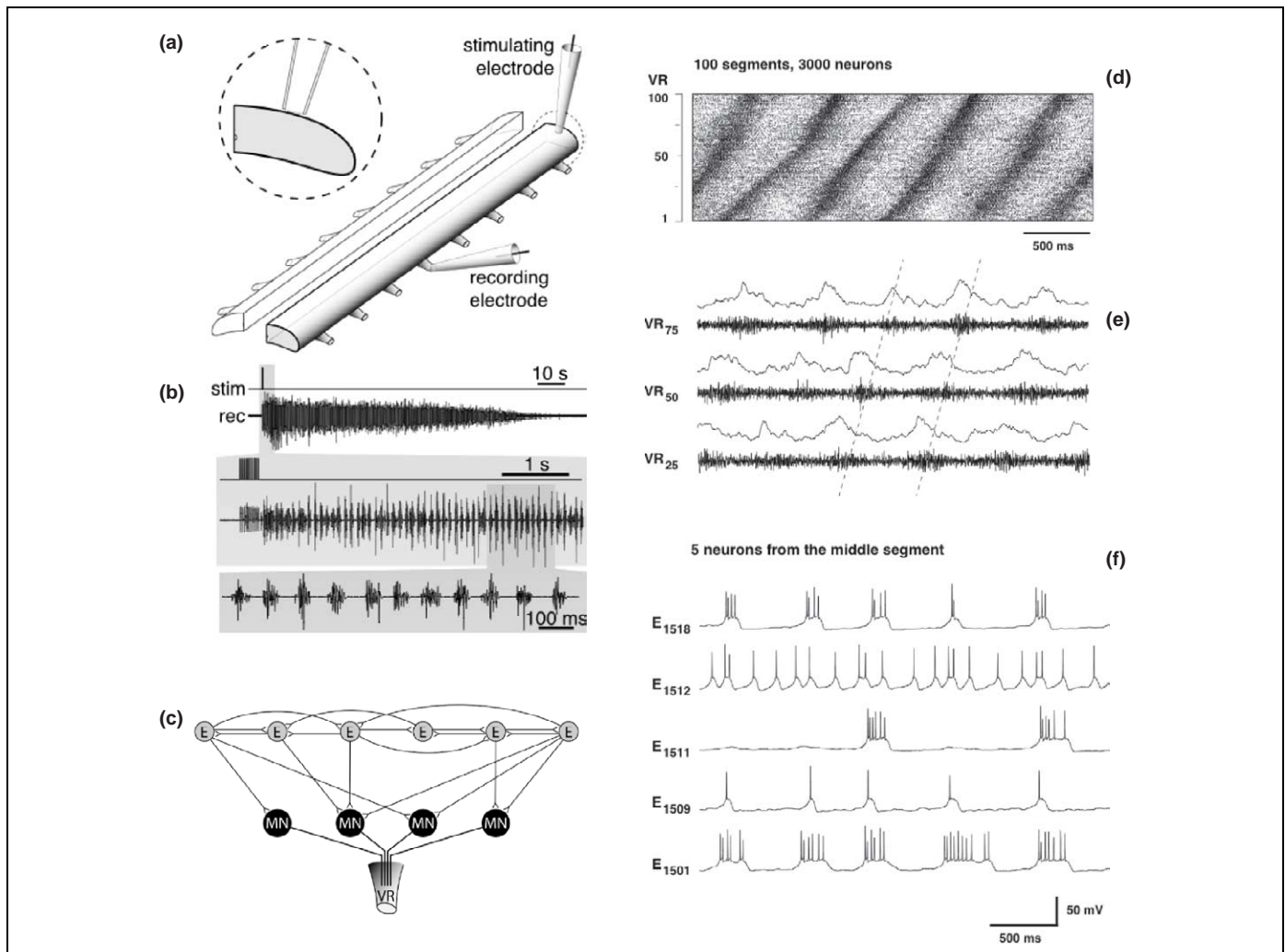
Figure 2. Large-scale CPG simulation of lamprey hemicord. On the left (a–c) are experimental data, and on the right are results from simulation of a full-scale model of the excitatory interneuron network. The network comprises 3000 conductance-based model neurons and >110 000 glutamatergic synapses. Activity during 3 s is shown. **(a)** A lamprey hemicord preparation rigged for electrical stimulation and recording of ventral root activity using pipette electrodes. **(b)** A brief train of pulses delivered via the stimulating electrode (stim) evokes a long bout of motor bursting at the ventral roots (rec). **(c)** A model network that accounts for the fast rhythmic bursting expressed by the hemicord. Only one hemisegment is shown, with the circles representing groups of neurons. Excitatory interneurons (E) form an interconnected network able to sustain repetitive firing by positive feedback, mediated by both fast ionotropic and slow metabotropic synaptic transmission. Fast synaptic interactions promote a certain degree of synchronization across the population. Phasic excitation is relayed to the motoneurons (MN). At each cycle, the individual action potentials from many motoneurons converge in the ventral root (VR) where a burst is recorded. **(d)** Spike raster plot of activity in all simulated ventral root neurons, numbered 1–100 rostrocaudally. The overall bursting pattern and 1%-per-segment phase lag can be seen. **(e)** Simulated average motoneuron membrane potential and ventral root recording synthesized from the model output, shown for three different segments. The delay of onset of consecutive bursts is marked with dashed lines. **(f)** Simulated membrane potential of five different excitatory interneurons in one of the middle segments. Model parameters for neurons and synaptic connectivity have significant random variability and therefore the activity of different neurons displays variable spike patterns. Data in (a–c) reproduced, with permission, from [22].

Bottom-up models and experiments based on studying the effect of excitatory glutamate agonists on network bursting frequency [15,23] suggested that the principal mechanism behind the intersegmental phase lag was the higher excitability in rostral segments [15]. However, top-down approaches pointed towards asymmetric synaptic coupling [24,25], because models using chains of coupled oscillators [25] better mimicked the behaviour of the spinal cord under conditions of mechanically forced oscillations [26].

Similar to our discussion of the leech intersegmental coordination [11], these divergent views partly emerged from experiments of a different nature that seemingly favoured one model over another. A current challenge is to unify the different theories and models so that progress can be made towards a more coherent view.

As already described, the underlying synaptic coupling is asymmetric, but its short-range components appear more important for effective intersegmental coordination, as demonstrated by abstract [27] and more detailed [16] computational models. To elucidate further the cellular and synaptic mechanisms behind intersegmental coordination, a biophysically detailed full-scale model of a reduced experimental preparation, the lamprey hemispinal cord, is currently being simulated (Figure 2d,e).

Incorporating neuromechanical models

The lamprey CPG is influenced by sensory feedback from the generated body undulations [15]. Can such interactions also be incorporated into the neuronal circuit models? More generally, can a model of a spinal pattern generator be connected to models of muscles and limbs to capture the entire movement-generation process?

Because all neural circuits have evolved to function in specific natural environments, any study, whether *in vitro*

or a simulation, in which the mechanical context is ignored might be severely limited. For example, function of the leg control circuits in stick-insect thoracic ganglia depends on feedback concerning mechanosensory variables such as joint position, velocity and strain [28]. From this perspective, the central goal is to replicate realistically the feedback received via mechanosensors, whereas other aspects of the movement produced is secondary.

Incorporating mechanical components into a simulation is not trivial. The mathematical models required for simulating body movements are different from those used when modelling neural activity and signalling. The interface between neurons and mechanical behaviour (i.e. muscles and mechanosensors) must therefore be described by models compatible with both mathematical languages. For mammals, muscle models available in the literature can serve this task [29], whereas insects and lower vertebrates might require more research to come up with sufficiently accurate models. On the sensory side, the main obstacle is to find the transfer functions that relate mechanical action to the neural signal. When accurate feedback signals are not crucial, simple linear transfer functions might suffice; otherwise, each variety of mechanosensor will require a specific model equation.

In a study of neuromechanical interactions in lamprey swimming [30], both muscles and mechanosensors were modelled as linear. The gross simplifications made when describing variables such as body mechanics and interactions with surrounding water made it irrelevant to incorporate more subtle models. Similar approaches have been successful in simulating both swimming and walking behaviour of the salamander [31]. In studies of walking in cats, more accurate models of muscles and sensors have proven important in mimicking natural behaviour [32,33].

Interaction with subcellular modelling

Intracellular signalling cascades can change microcircuit computations by modifying the intrinsic properties of neurons or the strengths of synaptic connections. They are important in the homeostatic control of these properties [34] but, because the signalling processes involved are at present poorly understood, no detailed biophysical models exist. In future such models will have to bridge the gap in timescales between electrical neuronal activity (milliseconds to minutes) and homeostasis (days). Fortunately, solutions are being developed for multi-timescale modelling [4,35].

Signalling pathways can be activated by synaptic input and there is rapid growth in the number of models simulating this interaction. Some studies focus on information processing by biochemical pathways (e.g. temporal computation [36,37]) but most simulate the induction of synaptic plasticity in the hippocampus or the cerebellum. Here, we review the recent work on the cerebellum.

Classical conditioning of the eye-blink response is a form of associative learning that involves induction of long-term depression (LTD) of parallel fibre (PF) synapses onto cerebellar Purkinje cells [38]. LTD is induced by increased postsynaptic Ca^{2+} concentration, caused by PF-evoked Ca^{2+} release from stores. It is assumed that this release is potentiated by voltage-gated Ca^{2+} influx

activated by preceding climbing-fibre input [39]. Several models simulating the complex intracellular signalling cascades involved have explored whether this mechanism is sufficient for acquisition of learning [40–42]. These models confirmed that the kinetics of biochemical interactions leading to Ca^{2+}-evoked protein kinase C (PKC) activation [38] could explain the temporal sensitivity during the learning phase [41]. They also indicated that additional mechanisms, such as a mitogen-activated protein kinase (MAPK)-dependent positive-feedback loop, might be involved [42], and this was recently experimentally confirmed [43]. Furthermore, these models explored the effects of other sources of Ca^{2+} influx [40], such as the non-associative PF-induced voltage-gated influx [44] that could interfere with learning [45]. Finally, at the microcircuit level, they enable quantitative comparison of models in which biochemical mechanisms are responsible for learning the timing delay of the conditioned response [46] with models that put this learning at the network level [47].

Interaction with cellular modelling

Most microcircuit models consist of networks of point neurons [1,2] (see Grillner et al. in this issue). But because dendritic integration of synaptic input [48] can have a strong effect on neuronal input–output function, there is growing interest in incorporating morphologically realistic models of neurons into microcircuit models. The standard technology for modelling dendrites is compartmental modelling with active conductances [3] but using this in microcircuit models introduces several challenges.

First, several models might need to be created, each requiring tens or hundreds of poorly constrained parameters. In the past these parameters have often been laboriously hand-tuned [49] but advances in optimization technologies make automatic parameter searches an attractive alternative. In general, evolutionary strategies [50], which are better suited for real-number parameters than genetic algorithms, outperform other methods in high-dimensional problems [51] and give better results in the presence of noise [52] – two important issues in neural modelling. An additional advantage of these methods is that they produce multiple possible solutions, which corresponds to the large variability found in real neurons [53,54].

This brings us to the second challenge: variability of neuronal morphology. In network modelling it is well known that introducing heterogeneity of neuron models can cause new dynamic modes to appear [55] and such networks are often less susceptible to noise than homogeneous ones [56,57]. In networks using simple neuron models, heterogeneity can be introduced as variability of the leak current or of voltage-gated channel densities. When more detailed models are used, one also has to consider variability in neuronal morphology. Unfortunately, for most neurons, only a few reconstructed morphologies are available and it requires much work [58] to add more samples. Nevertheless this approach, taken by the Blue Brain project, which plans to create a morphological realistic model of a complete cortical column (http://bluebrainproject.epfl.ch/), might be preferred over aggregating reconstructions from many

different laboratories. Several recent modelling studies showed that inter-laboratory differences in experimental methods cause so much divergence in neuronal reconstruction that, functionally, the data could be from different types of neuron [59,60] (Figure 3). Instead of using real reconstructions, one can also generate [61] or grow [62] random dendritic morphologies based on accurate statistical descriptions of the dendrites modelled. Although this might be ultimately the most rewarding approach, it has not yet been evaluated in realistic microcircuit simulations.

The third problem is synaptic wiring. To understand the morphological distribution of connections one must also reconstruct the axons of stained neurons. In some cases, for example invertebrate neurons where the spike initiation sites are in the axon (Figure 1b), one might have to model the axons completely. Fortunately, delay lines [57,63] can be used in most microcircuit models; using these, the time of arrival of a spike at each synapse is computed without simulating spike propagation. Connecting the neurons requires custom code for each type of axon modelled [64], because there are no general models specifying connectivity rules at the morphological scale. Additionally, the currents simulated must be those generated by single synaptic contacts rather than compound synaptic currents, which are simulated in most microcircuit models. In the simplest case this requires adapting the synaptic conductances used [64,65]. Regrettably, most microcircuit models are sub-sampled networks – that is, not all neurons are represented and substantial synaptic input is lacking. In single-neuron models one can compensate for absent presynaptic neurons by manipulating firing frequencies of input lines [66], but in microcircuits one can increase only the available synaptic conductances. When using real morphologies this is limited by the possible saturation of synaptic currents because of the high local input impedance of small dendritic branches and spines. Therefore the best, but also computationally most demanding, approach might be to go for full-scale modelling (see the following section), where all presynaptic neurons in the microcircuit are represented.

Interaction with large-scale network modelling

A microcircuit is, by definition, a component of a much larger network. It can be simulated to some degree in isolation, especially when it can be related to a reduced *in vitro* preparation such as a piece of lamprey spinal cord. But often it is in reality embedded in a mosaic of similar modules that requires large-scale network modelling. A major benefit of a large-scale model is that, by providing a realistic number of presynaptic inputs, it removes the need to increase synaptic connection probabilities or conductances [63]. Such compensations tend to distort significantly the dynamics of the network.

Fortunately, one reason for avoiding large-scale simulations is gradually disappearing. Although the reduction of dimensions and increase of clock frequencies of integrated circuits might be approaching their limits, the number of processors operating in parallel in next-generation computers will increase dramatically. Because neuronal networks represent homogenous computational structures, parallel simulation is relatively straightforward [67] (P. Hammarlund, PhD thesis, Royal Institute of Technology, Stockholm, 1996). Thus, in the near future, computer power might no longer prevent us from putting together and studying large and even full-scale models of whole-brain networks.
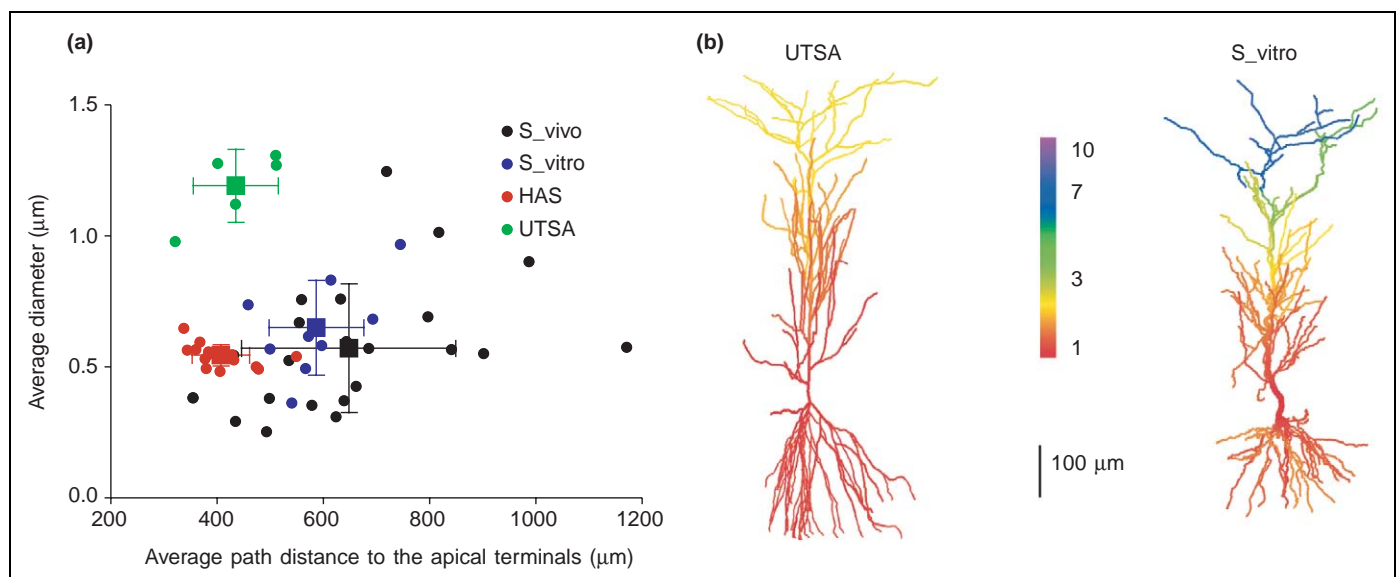
Figure 3. Difference in properties of archived neuron reconstructions. The morphological properties of CA1 hippocampal pyramidal neurons measured on reconstructions obtained from three different internet archives: 'S_vivo' and 'S_vitro' data are from the Duke/Southampton archive of neuronal morphology (http://neuron.duke.edu/cells/cellarchive.html), 'HAS' data are from the Hungarian Academy of Sciences archive (http://ux.koki.hu/~gulyas/ca1cells/cellfiles.htm) and 'UTSA' data are from the University of Texas at San Antonio archive (http://www.utsa.edu/claibornelab/) [60]. **(a)** Quantitative morphometric differences between cell groups shown as the relationship between size of the cells (*x*-axis) and the average diameter of their dendrites (*y*-axis). Each data point represents one cell, and the population means ±1 SD are shown. **(b)** The large morphometric differences have functional consequences: simulated localization-dependent attenuation of inhibitory postsynaptic currents show that the neuron on the right (from the S_vitro group) attenuates synaptic current much more than the one on the left (from the UTSA archive). Colours code the attenuation at the site of the synapse, which is computed as the ratio of maximum amplitude of synaptic current at this site to amplitude in the soma. Somata are not drawn and diameters of the S_vitro cell are drawn at a scale three-times greater than those of the UTSA cell, to enhance visibility. Panel (a) is modified, with permission, from [60].

Of course, the number of under-constrained parameters increases when going from a small to a much larger network model. Currently, parallel simulation of networks of millions of neurons and billions of synapses can be performed on large cluster computers. Such models include several billion parameters. Fortunately, neuronal networks are typically described as comprising a limited number of cell types, with basically the same properties but some variation within the population. The parameter used for one neuron of a certain type can also be used for the others, possibly with a compact description of a distribution around a mean (Figure 2f). This holds also for the synaptic interactions. Moreover, synaptic conductances are not determined arbitrarily but are the result of genetic specification interacting with plasticity and learning rules that couple them to historical network activity [68]. In practice, the number of truly free parameters is therefore more or less independent of the actual number of neurons and synapses in the network.

Further, somewhat counter-intuitively, for very large networks there is little extra cost to simulating complex neuron models. Contrary to the case for single neurons and small networks, the solution methods used for dendritic integration [69] do not add significantly to simulation time, because synaptic computation dominates, owing to the large number of contacts modelled. Fortunately, the spiking communication between neurons often does not require fast inter-processor communication, which can be a problem in parallel cluster computing. As long as neurons only interact with spiking events over delay lines, communication can be based on 'address event representation' [67] and parallel neural simulation is bound by local computation. As soon as continuous cell–cell interactions such as electrotonic synapses or graded transmitter release (Figure 1) need to be simulated, parallel simulations have to be organized differently and the communication overheads become potentially performance-limiting.

Concluding remarks

Quantitative computational modelling has come to neuroscience to stay. As these techniques become increasingly integrated with experimental research, there will be more knowledge extracted from existing experimental data and model predictions will enter more routinely into the planning of new experiments. But to succeed, better integration of bottom-up modelling, which will rapidly increase in detail because of affordable massively parallel computers, with top-down approaches is needed.

References
1 Marder, E. and Calabrese, R.L. (1996) Principles of rhythmic motor pattern generation. *Physiol. Rev.* 76, 687–717
2 Whittington, M.A. and Traub, R.D. (2003) *Interneuron Diversity series:* inhibitory interneurons and network oscillations *in vitro. Trends Neurosci.* 26, 676–682
3 De Schutter, E. and Steuber, V. (2000) Modeling simple and complex active neurons. In *Computational Neuroscience: Realistic Modeling for Experimentalists* (De Schutter, E., ed.), pp. 233–257, CRC Press
4 Cannon, R.C. *et al.* (2003) From biophysics to behavior: Catacomb2 and the design of biologically-plausible models for spatial navigation. *Neuroinformatics* 1, 3–42
5 Cymbalyuk, G. *et al.* (2002) Bursting in leech heart interneurons: cell-autonomous and network-based mechanisms. *J. Neurosci.* 22, 10580–10592
6 De Schutter, E. *et al.* (1993) A model of graded synaptic transmission for use in dynamic network simulations. *J. Neurophysiol.* 69, 1225–1235
7 Hill, A.A. *et al.* (2001) A model of a segmental oscillator in the leech heartbeat neuronal network. *J. Comput. Neurosci.* 10, 281–302
8 Nadim, F. *et al.* (1995) Modeling the leech heartbeat elemental oscillator. I. Interactions of intrinsic and synaptic currents. *J. Comput. Neurosci.* 2, 215–235
9 Olsen, Ø.H. and Calabrese, R.L. (1996) Activation of intrinsic and synaptic currents in leech heart interneurons by realistic waveforms. *J. Neurosci.* 16, 4958–4970
10 Hill, A.A. *et al.* (2002) Model of intersegmental coordination in the leech heartbeat neuronal network. *J. Neurophysiol.* 87, 1586–1602
11 Jezzini, S.H. *et al.* (2004) Detailed model of intersegmental coordination in the timing network of the leech heartbeat central pattern generator. *J. Neurophysiol.* 91, 958–977
12 Masino, M.A. and Calabrese, R.L. (2002) A functional asymmetry in the leech heartbeat timing network is revealed by driving the network across various cycle periods. *J. Neurosci.* 22, 4418–4427
13 Shilnikov, A. *et al.* (2005) Mechanism of bistability: tonic spiking and bursting in a neuron model. *Phys. Rev. E* 71, 056214
14 Izhikevich, E.M. *Dynamical Systems in Neurosciences: the Geometry of Excitability and Bursting*, MIT Press (in press)
15 Grillner, S. (2003) The motor infrastructure: from ion channels to neuronal networks. *Nat. Rev. Neurosci.* 4, 573–586
16 Kotaleski, J.H. *et al.* (1999) Neural mechanisms potentially contributing to the intersegmental phase lag in lamprey.I. Segmental oscillations dependent on reciprocal inhibition. *Biol. Cybern.* 81, 317–330
17 Kotaleski, J.H. *et al.* (1999) Neural mechanisms potentially contributing to the intersegmental phase lag in lamprey.II. Hemisegmental oscillations produced by mutually coupled excitatory neurons. *Biol. Cybern.* 81, 299–315
18 Kozlov, A.K. *et al.* (2002) Mechanisms for lateral turns in lamprey in response to descending unilateral commands: a modeling study. *Biol. Cybern.* 86, 1–14
19 Kozlov, A. *et al.* (2001) Modeling of substance P and 5-HT induced synaptic plasticity in the lamprey spinal CPG: consequences for network pattern generation. *J. Comput. Neurosci.* 11, 183–200
20 Lansner, A. *et al.* (1997) Realistic modeling of burst generation and swimming in lamprey. In *Neurons, Networks, and Motor Behavior* (Stein, P.S.G., and Al., E., eds), pp. 165–171, MIT Press
21 Cangiano, L. and Grillner, S. (2003) Fast and slow locomotor burst generation in the hemispinal cord of the lamprey. *J. Neurophysiol.* 89, 2931–2942
22 Cangiano, L. and Grillner, S. (2005) Mechanisms of rhythm generation in a spinal locomotor network deprived of crossed connections: the lamprey hemicord. *J. Neurosci.* 25, 923–935
23 Matsushima, T. and Grillner, S. (1992) Neural mechanisms of intersegmental coordination in lamprey: local excitability changes modify the phase coupling along the spinal cord. *J. Neurophysiol.* 67, 373–388
24 Cohen, A.H. *et al.* (1992) Modelling of intersegmental coordination in the lamprey central pattern generator for locomotion. *Trends Neurosci.* 15, 434–438
25 Kopell, N. (1995) Chains of coupled oscillators. In *The Handbook of Brain Theory and Neural Networks* (Arbib, M.A., ed.), pp. 178–183, MIT Press
26 Sigvardt, K.A. and Williams, T.L. (1996) Effects of local oscillator frequency on intersegmental coordination in the lamprey CPG: theory and experiment. *J. Neurophysiol.* 76, 4094–4103
27 Ullström, M. *et al.* (1998) Activity-dependent modulation of adaptation produces a constant burst proportion in a model of the lamprey spinal locomotor generator. *Biol. Cybern.* 79, 1–14

28 Ekeberg, Ö. *et al*. (2004) Dynamic simulation of insect walking. *Arthropod Struct. Dev.* 33, 287–300

29 Zajac, F.E. (1989) Muscle and tendon – properties, models, scaling, and application to biomechanics and motor control. *Crit. Rev. Biomed. Eng.* 17, 359–411

30 Ekeberg, Ö. (1993) A combined neuronal and mechanical model of fish swimming. *Biol. Cybern.* 69, 363–374

31 Ijspeert, A.J. (2001) A connectionist central pattern generator for the aquatic and terrestrial gaits of a simulated salamander. *Biol. Cybern.* 84, 331–348

32 Ekeberg Ö. and Pearson K.G. Computer simulation of stepping in the hind legs of the cat: an examination of mechanisms regulating the stance-to-swing transition. *J. Neurophysiol.* (in press)

33 Yakovenko, S. *et al*. (2004) Contribution of stretch reflexes to locomotor control: a modeling study. *Biol. Cybern.* 90, 146–155

34 Turrigiano, G.G. and Nelson, S.B. (2004) Homeostatic plasticity in the developing nervous system. *Nat. Rev. Neurosci.* 5, 97–107

35 Takahashi, K. *et al*. (2004) A multi-algorithm, multi-timescale method for cell simulation. *Bioinformatics* 20, 538–546

36 Ajay, S.M. and Bhalla, U.S. (2004) A role for ERKII in synaptic pattern selectivity on the time-scale of minutes. *Eur. J. Neurosci.* 20, 2671–2680

37 Bhalla, U.S. (2002) Biochemical signaling networks decode temporal patterns of synaptic input. *J. Comput. Neurosci.* 13, 49–62

38 Ito, M. (2001) Cerebellar long-term depression: characterization, signal transduction, and functional roles. *Physiol. Rev.* 81, 1143–1195

39 Wang, S.S-H. *et al*. (2000) Coincidence detection in single spines mediated by calcium release. *Nat. Neurosci.* 3, 1266–1273

40 Doi, T. *et al*. (2005) Inositol 1,4,5-trisphosphate-dependent Ca^{2+} threshold dynamics detect spike timing in cerebellar Purkinje cells. *J. Neurosci.* 25, 950–961

41 Kotaleski, J.H. *et al*. (2002) Subcellular interactions between parallel fibre and climbing fibre signals in Purkinje cells predict sensitivity of classical conditioning to interstimulus interval. *Integr. Physiol. Behav. Sci.* 37, 265–292

42 Kuroda, S. *et al*. (2001) Exploration of signal transduction pathways in cerebellar long-term depression by kinetic simulation. *J. Neurosci.* 21, 5693–5702

43 Yamamoto, K. *et al*. (2003) Sequence of signal transduction events involved in induction of cerebellar long-term depression. Program number 170.2 In *2003 Abstract Viewer and Itinerary Planner*, Society for Neuroscience, online (http://sfn.scholarone.com/)

44 Hartell, N.A. (1996) Strong activation of parallel fibers produces localized calcium transients and a form of LTD that spreads to distant synapses. *Neuron* 16, 601–610

45 De Schutter, E. (1995) Cerebellar long-term depression might normalize excitation of Purkinje cells: a hypothesis. *Trends Neurosci.* 18, 291–295

46 Steuber, V. and Willshaw, D. (2004) A biophysical model of synaptic delay learning and temporal pattern recognition in a cerebellar Purkinje cell. *J. Comput. Neurosci.* 17, 149–164

47 Ohyama, T. *et al*. (2003) What the cerebellum computes. *Trends Neurosci.* 26, 222–227

48 Hausser, M. and Mel, B. (2003) Dendrites: bug or feature? *Curr. Opin. Neurobiol.* 13, 372–383

49 De Schutter, E. and Bower, J.M. (1994) An active membrane model of the cerebellar Purkinje cell. I. Simulation of current clamps in slice. *J. Neurophysiol.* 71, 375–400

50 Eiben, A.E. and Smith, J.E. (2003) *Introduction to Evolutionary Computing*, Springer-Verlag

51 Moles, C.G. *et al*. (2003) Parameter estimation in biochemical pathways: a comparison of global optimization methods. *Genome Res.* 13, 2467–2474

52 Krink, T. *et al*. (2004) Noisy optimization problems – a particular challenge for differential evolution? In *Congress on Evolutionary Computation, 2004*, pp. 332–339, IEEE Press

53 Golowasch, J. *et al*. (2002) Failure of averaging in the construction of a conductance-based neuron model. *J. Neurophysiol.* 87, 1129–1131

54 Swensen, A.M. and Bean, B.P. (2005) Robustness of burst firing in dissociated Purkinje neurons with acute or long-term reductions in sodium conductance. *J. Neurosci.* 25, 3509–3520

55 Golomb, D. and Rinzel, J. (1993) Dynamics of globally coupled inhibitory neurons with heterogeneity. *Phys. Rev. E Stat. Phys. Plasmas Fluids Relat. Interdiscip. Topics* 48, 4810–4814

56 Bartos, M. *et al*. (2002) Fast synaptic inhibition promotes synchronized gamma oscillations in hippocampal interneuron networks. *Proc. Natl. Acad. Sci. U. S. A.* 99, 13222–13227

57 Maex, R. and De Schutter, E. (2003) Resonant synchronization in heterogeneous networks of inhibitory neurons. *J. Neurosci.* 23, 10503–10514

58 Jaeger, D. (2000) Accurate reconstruction of neuronal morphology. In *Computational Neuroscience: Realistic Modeling for Experimentalists* (De Schutter, E., ed.), pp. 159–178, CRC Press

59 Scorcioni, R. *et al*. (2004) Quantitative morphometry of hippocampal pyramidal cells: differences between anatomical classes and reconstructing laboratories. *J. Comp. Neurol.* 473, 177–193

60 Szilagyi, T. and De Schutter, E. (2004) Effects of variability in anatomical reconstruction techniques on models of synaptic integration by dendrites: a comparison of three Internet archives. *Eur. J. Neurosci.* 19, 1257–1266

61 Ascoli, G.A. *et al*. (2001) Generation, description and storage of dendritic morphology data. *Philos. Trans. R. Soc. Lond. B Biol. Sci.* 356, 1131–1145

62 van Pelt, J. and Uylings, H.B. (2002) Branching rates and growth functions in the outgrowth of dendritic branching patterns. *Network* 13, 261–281

63 Hasselmo, M.E. and Kapur, A. (2000) Modeling of large networks. In *Computational Neuroscience: Realistic Modeling for Experimentalists* (De Schutter, E., ed.), pp. 289–315, CRC Press

64 Solinas, S. *et al*. (2003) Synchronization of Purkinje cell pairs along the parallel fiber axis: a model. *Neurocomput.* 57, 97–102

65 Solinas, S. *et al*. (2004) Amplification of inhibitory postsynaptic potentials in a Purkinje cell model. *FENS Forum Abstr.* 2, A012.021 (http://fens2004.neurosciences.asso.fr/)

66 Jaeger, D. *et al*. (1997) The role of synaptic and voltage-gated currents in the control of Purkinje cell spiking: a modeling study. *J. Neurosci.* 17, 91–106

67 Goddard, N. *et al*. (2001) Neosim: portable plug and play neuronal modelling. *Neurocomput.* 40, 1657–1661

68 Bednar, J.A. *et al*. (2004) Scaling self-organizing maps to model large cortical networks. *Neuroinformatics* 2, 275–302

69 Mascagni, M.V. and Sherman, A.S. (1998) Numerical methods for neuronal modeling. In *Methods in Neuronal Modeling: from Ions to Networks* (2nd edn) (Koch, C. and Segev, I., eds), pp. 569–606, MIT Press